

## p(AAm/TA)-based IPN hydrogel films with antimicrobial and antioxidant properties for biomedical applications

Mehtap Sahiner,<sup>1</sup> Selin Sagbas,<sup>2</sup> Behzat Oral Bitlisli<sup>1</sup>

<sup>1</sup>Leather Engineering Department, Engineering Faculty, Ege University, 35100 Bornova Izmir, Turkey

<sup>2</sup>Chemistry Department, Faculty of Science & Arts, Canakkale Onsekiz Mart University, 17100 Canakkale, Turkey

Correspondence to: B. O. Bitlisli (E-mail: Behzatbitlisli@gmail.com)

**ABSTRACT:** Interpenetrating polymer networks (IPN), either semi-IPN (s-IPN) or full IPN, based on a natural polymer tannic acid (TA) and synthetic poly(acrylamide) (p(AAm)) were prepared by incorporation of TA during p(AAm) hydrogel film preparation with and without crosslinking of TA simultaneously. The synthesis of p(AAm/TA) s-IPN and IPN hydrogels with different amounts of TA were prepared by concurrent use of redox polymerization and epoxy crosslinking. The p(AAm)-based hydrogels were completely degraded at 37.5°C within 9 and 2 days at pHs 7.4 and 9, respectively. Biocompatibility of p(AAm), s-IPN, and IPN were tested with WST assay and double staining, they had 75% cell viability up to almost 20  $\mu\text{g mL}^{-1}$  concentration against L929 fibroblast cell. Antioxidant properties of IPN and s-IPN hydrogels were investigated with FC and ABTS<sup>-</sup> methods. Antimicrobial properties of TA-containing s-IPN, and IPN hydrogels were determined against three common bacterial strains, *Escherichia coli* ATCC 8739, *Staphylococcus aureus* ATCC 6538, and *Bacillus subtilis* ATCC 6633, and it was found that p(AAm/TA)-based s-IPN and IPN hydrogels are effective antimicrobial and antioxidant materials. Moreover, almost up to day-long linear TA release profiles were obtained from IPN and s-IPN hydrogels in phosphate buffer solution at pH 7.4 at 37.5°C. © 2015 Wiley Periodicals, Inc. *J. Appl. Polym. Sci.* **2015**, *132*, 41876.

**KEYWORDS:** biomedical applications; biomaterials; drug delivery systems; gels; hydrophilic polymers

Received 6 September 2014; accepted 12 December 2014

DOI: 10.1002/app.41876

### INTRODUCTION

Hydrogels, that swell in aqueous medium, can be considered soft and flexible, viscoelastic crosslinked materials and possess appropriate physical properties for wound healing dressing applications.<sup>1,2</sup> Interpenetrating polymeric networks (IPN) have two independent polymers forming intertwined networks and are prepared by nonintervening polymerization and crosslinking. On the other hand, semi-interpreting networks (s-IPN) are also polymer networks that contain another linear polymer entangled with the crosslinked network structure. The components of IPN and s-IPN hydrogels are not bound to each other chemically but the first is an inseparable combination of two polymers as they are independently crosslinked, while in the second (s-IPN) the linear polymer chains can be eluted from the network.<sup>3</sup> Therefore, IPN structures, especially in hydrogel film forms, provide great opportunity due to the additive effect of the polymers within the multicomponent polymeric system.<sup>4</sup>

Wounds are generally physical injuries of the skin and healing is a complex process initiated in response to an injury to restore function.<sup>5</sup> Wound healing is an extensive biological process, as degradation has occurred reassembly of connective tissue and

epidermal layers is necessary. In wound healing three processes occur: first inflammation, then granulation and finally spontaneous re-epithelialization.<sup>6</sup> Therefore, the materials that are used as the dressing for wounds are very important from pharmaceutical and medical application points of view. In the past, conventional materials used in wound healing were simple synthetic or natural bandages such as cotton wool, lint, gauzes, etc. The functions of these bandages were to (1) prevent bacterial activity around the wound and (2) keep the wound dry by allowing evaporation of the wound exudates.<sup>7</sup> Wound or burn healing processes necessitate wound fluid absorption, and negative pressure,<sup>8</sup> preventing infections, maintaining skin debridement of the necrotic tissue, and elasticity, adhesive and antimicrobial properties,<sup>9</sup> biocompatibility and biodegradability, oxygen permeability,<sup>10</sup> water vapor permeability,<sup>11</sup> maintaining suitable moisture around the wound,<sup>1</sup> and easy and extensive storage capability of therapeutic agents.<sup>8,11</sup> Therefore, IPN and s-IPN hydrogels by suitable choice of their components can be used as scaffolds for soft tissue, because of their tunable properties such as biocompatibility, biodegradability, and biomimicry of extra cellular matrices and adaptable mechanical properties. IPN hydrogels have many applications in diverse biomedical

fields as activation agent delivery systems, tissue engineering templates, artificial organs, wound dressing, and so on.

Polyphenolics are known as antimicrobial and antioxidant materials that scavenge free radicals.<sup>12</sup> Tannic acid (TA) is a natural plant-based polyphenolic compound, and exhibits diverse biological functions such as antioxidant, antimicrobial, astringent, homeostatic, antimutagenic, antiviral, and anti-inflammatory properties.<sup>5,13–15</sup> Therefore, in this investigation, TA-containing p(AAm) hydrogel composites in the forms of s-IPN and IPN were prepared and characterized. It was reported that p(AAm) hydrogels have many applications, and are nontoxic, with good swelling properties, and have ready gelation property.<sup>15–17</sup> p(AAm), and p(AAm/TA) s-IPN hydrogels were synthesized with redox polymerization technique whereas p(AAm/TA) IPN hydrogels were prepared by concurrent redox polymerization and epoxy crosslinking reactions. The maximum swelling properties of the hydrogels at different solution pHs (pH 4, 5.5, 7.4) at 37.5°C, and physicochemical and biological properties were investigated to evaluate their potential usefulness as wound healing materials. Biodegradability is an important factor for wound healing, as the degradability of the materials can inhibit the proliferation of keloid fibroblasts, resulting in acceleration of wound healing,<sup>18</sup> and as TA is known as a therapeutic agent for biological systems it can be released from the IPN structure to perform the same task. Therefore, thermal degradation and degradability of hydrogel IPNs at different pHs were investigated at 37.5°C. p(AAm/TA) s-IPN (containing different amounts of TA), and p(AAm/TA) IPN hydrogels with different amounts of crosslinker were tested for controlled TA release studies in phosphate-buffered saline (PBS; pH 7.4) at 37.5°C. Furthermore, antioxidant and antimicrobial properties of TA-containing s-IPN and IPN hydrogels were determined. Biocompatibilities of the IPN hydrogels were also investigated with WST assay and double staining methods.

## MATERIALS AND METHODS

### Materials

Acrylamide (Merck, 99%) and tannic acid (TA; ACS grade, Mn: 1700.2 g/mol, Sigma Aldrich) as biological polyphenol or oligomers, poly(ethylene glycol) diacrylate (p(EGDA), Aldrich) with molecular weight Mn: 258 g/mol and technical grade trimethylolpropane triglycidyl ether (TMPGDE, Aldrich) as crosslinkers were used. Ammonium persulfate (APS, 97% Sigma-Aldrich) as redox initiator and N,N,N',N'-tetramethylethylenediamine (TEMED, Acros) as an accelerator were used. NaOH (Merck) and HCl (37.5–38% Aldrich) were used. Folin-Ciocalteu's phenol reagent (FC) (Sigma-Aldrich), 2,2'-Azino-bis-(3-ethylbenzothiazoline-6-sulfonic acid) (ABTS, Aldrich), and gallic acid (GA) (97.5–102.5%, Aldrich) were used for antioxidant studies. *Escherichia coli* ATCC 8739, *Staphylococcus aureus* ATCC 6538, and *Bacillus subtilis* ATCC 6633 strains were used for antimicrobial tests. Nutrient agar (Merck) and nutrient broth (Merck) were used as microbial growth media. L929 Fibroblast cell lines were purchased from SAP Institute of the Ministry of Agriculture (Ankara, Turkey). Cell culture flasks and other plastic materials were purchased from Corning (NY). Dulbecco Modified Eagle's Medium (DMEM) with L-glutamine,

fetal calf serum (FCS), Trypsin-EDTA, hoechst 33342, and propidium iodide (PI) were purchased from Serva (Israel), and WST-1 [2-(4-iodophenyl)-3-(4-nitrophenyl)-5-(2,4-disulphophenyl)-2H-tetrazolium] reagent was purchased from Roche (Germany). All aqueous solutions were freshly prepared using ultra pure 18.2 MΩ cm distilled water (DI; Millipore-Direct Q UV3).

### Synthesis of IPN Hydrogels

**Synthesis of p(AAm) Hydrogel.** Bulk p(AAm) hydrogel film was prepared by a simple redox polymerization technique. AAm, 1 g, was dissolved in 2 mL water by vortex mixing. Then, 0.5 mol % p(EGDA), 0.5 mL of 0.5 mol % APS (based on monomer), and 5 μL TEMED were added into the mixture. The hydrogel precursor solution was placed in 2 × 2.5 cm glass cups, and the polymerization and crosslinking reaction continued for 12 h at room temperature. Then, the gel was cut into 6 mm cylindrical shapes with a cutter, and immersed in DI water for 12 h to remove the impurities. Lastly, the hydrogels were dried in oven until no weight changes was observed at 40°C.

**Synthesis of p(AAm/TA) Semi-IPN Hydrogels.** p(AAm/TA) semi-IPN hydrogels were synthesized via a free radical polymerization technique. Briefly, 1 g AAm and different amounts of TA (0.025, 0.05, 0.1, and 0.15 g as TA, 2TA, 4TA, 6TA) were dissolved in 1 mL distilled water and vortex mixed for synthesis of p(AAm/TA), p(AAm/2TA), p(AAm/4TA), and p(AAm/6TA) as s-IPN hydrogels, respectively. Crosslinker and initiator amounts were changed according to the amount of TA. Different amounts (0.1, 0.25, 0.5, and 1 mol %) of p(EGDA) and 0.5 mL of 0.5–1 mol % APS (with respect to total monomer amount) were added to the monomer mixture for TA, 2TA, 4TA, and 6TA, respectively. Immediately, 10–20 μL of TEMED was added into the mixture as accelerator and vortexed. The precursor solutions were placed in 2 cm × 2.5 cm glass cups and the polymerizations and the crosslinking reactions were allowed to take place simultaneously for 12 h at ambient temperature. The s-IPN hydrogels were cut in 6 mm cylindrical shapes and washed with excess amounts of DI water for 12 h. The hydrogels were dried in an oven to a constant weight at 40°C and kept in a closed container for further use.

**Synthesis of p(AAm/TA) IPN Hydrogels.** p(AAm/TA) IPN hydrogel was synthesized via radical polymerization and epoxy crosslinking simultaneously. In short, AAm, 1 g, and TA, 0.15 g, were dissolved in 1 mL distilled water and vortex mixed to form an isotropic solution. Then, 1 mol % p(EGDA) crosslinker for AAm and 0.5 mL of 1 mol % APS were added to the monomer mixture. The other crosslinker, TMPGDE (3.26 or 6.52 mol %) for TA was added to the mixtures to synthesize p(AAm/TA)-X (X: 3.26 mol % TMPGDE) and p(AAm/TA)-2X IPN hydrogels, respectively. Immediately, 10 μL of TEMED was added to the mixtures. The precursor solutions were injected into plastic pipettes and then placed in a 70°C oven for polymerization and crosslinking reactions to take place simultaneously over 12 h. Prepared p(AAm/TA) IPN hydrogels containing X and 2X crosslinkers were removed from their plastic pipettes, cut into 3–4 mm cylindrical shapes and washed with DI water overnight. The

**Table I.** The Amount of Tannic Acid (TA), Initiator, and the Crosslinkers for 1 g AAm Used in the Polymerization and Crosslinking Reactions, and Their Amounts After Drying to Constant Weight

Concentration of hydrogel ( $\mu\text{g mL}^{-1}$ )	TA X IPN		6TA s-IPN		p(AAm)	
	% apoptosis	% necrosis	% apoptosis	% necrosis	% apoptosis	% necrosis
0	$1.0 \pm 1.0$	$1.0 \pm 0.5$	$1.0 \pm 1.0$	$1.0 \pm 0.5$	$1.0 \pm 1.0$	$1.0 \pm 0.5$
4.6	$5.0 \pm 0.5$	$15.0 \pm 1.0$	$4.5 \pm 0.8$	$13.5 \pm 1.0$	$4.0 \pm 1.4$	$1.5 \pm 1.0$
9.37	$7.0 \pm 1.0$	$22.5 \pm 2.0$	$6.0 \pm 1.5$	$16.0 \pm 0.7$	$6.5 \pm 1.0$	$5.0 \pm 0.7$
18.75	$8.0 \pm 0.7$	$25.5 \pm 1.0$	$7.0 \pm 2.0$	$22.0 \pm 0.5$	$7.0 \pm 0.7$	$8.5 \pm 2.0$
37.5	$8.5 \pm 2.0$	$27.0 \pm 0.8$	$8.0 \pm 1.2$	$28.5 \pm 2.0$	$8.5 \pm 2.0$	$15.0 \pm 1.4$
75	$10.0 \pm 1.4$	$32 \pm 0.5$	$9.5 \pm 1.0$	$30.0 \pm 0.8$	$9.0 \pm 1.5$	$23.5 \pm 1.0$
150	$15.0 \pm 0.6$	$39.5 \pm 1.0$	$11 \pm 0.5$	$34.5 \pm 1.0$	$13.0 \pm 2.0$	$30.0 \pm 1.5$

cleaned hydrogels were dried in an oven to a constant weight at  $40^\circ\text{C}$  and kept in a closed container for further use. The details of the preparation of all the hydrogel matrices are given in Table I.

#### Characterization of p(AAm), p(AAm/TA) s-IPN, and p(AAm/TA) IPN Hydrogels

The p(AAm/TA) IPN hydrogel was imaged by scanning electron microscope (SEM) by placing the freeze-dried sample onto carbon tape-attached aluminum SEM stubs, after coating with gold to a thickness of a few nanometers in a vacuum using an SEM (Jeol JSM-5600 LV), operating at 20 kV.

The thermal characterization of p(AAm), p(AAm/TA) s-IPN, and p(AAm/TA) IPN hydrogels were carried out using a thermo gravimetric analyzer (SII TG/DTA 6300). About 5 mg of material was placed in a ceramic crucible and the weight lost was recorded over the temperature range of  $50\text{--}500^\circ\text{C}$  at a heating rate of  $10^\circ\text{C min}^{-1}$  under a dry flow of  $\text{N}_2$  of  $100\text{ mL min}^{-1}$ .

The functional groups of p(AAm)-based materials were determined using FT-IR spectroscopy (Perkin Elmer spectrum 100), in the spectral range of  $4000\text{--}650\text{ cm}^{-1}$  with a resolution of  $4\text{ cm}^{-1}$ , using the ATR technique.

The zeta potential of the granulated hydrogels (100 mg/50 mL) were measured with Zeta-Pals Zeta Potential Analyzer (Brookhaven Instrument Corp.) in 0.01 M KCl solutions at different pH's in DI water. The results are presented as the average values of 10 measurements. The effect of solution pH on hydrogel zeta potentials was also investigated by adjusting the granulated hydrogel-containing solutions (100 mg/50 mL) to different pH values between 2 and 10. The solution pH was adjusted using 0.2 M NaOH or HCl solution.

#### Swelling Properties of p(AAm), p(AAm/TA) s-IPN, and p(AAm/TA) IPN Hydrogels

Dried hydrogels were left to swell in different pH solutions in phosphate and citrate buffer, such as pH 4, 5.5, 7.4, and 9 at  $37.5^\circ\text{C}$  in a shaking water bath. Swollen hydrogels were removed from the water bath after 5 h for pH 9 and 3 days for pH 4, 5.5, and 7.4, blot dried with filter paper and weighed. The percentage maximum swelling,  $S_{\text{Max}}\%$ , was calculated from the following equation:

$$S_{\text{Max}}\% = [(M_t - M_0)/M_0] \times 100 \quad (1)$$

where  $M_0$ , is the mass of the dry gel at time 0 and  $M_t$ , is the mass of the swollen hydrogel after 3 days.

#### In Vitro Degradation of p(AAm), p(AAm/TA) s-IPN, and p(AAm/TA) IPN Hydrogels

In degradation studies, the mass decrease in p(AAm)-based hydrogels at pH 4 in citrate buffer, pH 5.4 in citrate buffer, pH 7.4 in PBS, and pH 9 in borate buffer were measured gravimetrically. In short, 50 mg hydrogels were placed into 40 mL pH solution at  $37.5^\circ\text{C}$  in a shaking water bath, and the weight loss of the hydrogels was determined by weighing at different times.

#### TA Release from p(AAm/TA) s-IPN and p(AAm/TA) IPN Hydrogels

The TA release from p(AAm/TA) IPN hydrogels with different amounts of crosslinkers (X and 2X) and p(AAm/TA) s-IPN hydrogels which have four different amounts of TA (TA, 2TA, 4TA, and 6TA) were compared. Briefly, 50 mg dried hydrogels were placed into 40 mL PBS (pH 7.4) at  $37.5^\circ\text{C}$  in a shaking water bath. The released amount of TA into the PBS buffer was determined with UV-Vis spectroscopy at 280 nm from previously constructed calibration curves at the same wavelengths for TA. The release measurements were performed in triplicate and the results are given as the average value with standard deviation.

**TA Release Kinetics.** For TA release studies from hydrogel matrices, linear and nonlinear mathematical models such as zero order, first order, Korsmeyer-Peppas and Higuchi kinetic models were compared. Zero order and first order models are expressed as eqs. (2) and (3), respectively.<sup>19</sup>

$$Q_t = Q_0 + k_0 t \quad (2)$$

$$\log Q_t = \log Q_0 + k_1 t / 2.303 \quad (3)$$

where  $Q_t$  is the amount of TA release in time  $t$ ,  $Q_0$  the initial amount of TA in solution,  $k_0$  (zero order) and  $k_1$  (first order) rate constants and  $t$  is the time.

Korsmeyer-Peppas and Higuchi models can be expressed as eqs. (3) and (4), respectively.<sup>19</sup>

$$M_t/M_\infty = kt^n \quad (4)$$

Where  $M_t/M_\infty$  is the fractional TA release,  $t$  is the release time,  $k$  is the constant related to drug/polymer structure and  $n$  is the

diffusional exponent. The value of  $n$  is used to determine the drug release mechanisms. When  $n \leq 0.45$ , the transport mechanism is indicated controllable drug release by Fickian diffusion. The value of  $n$  between  $0.45 < n < 0.89$  revealed that the anomalous or non-Fickian diffusion mechanism. When  $n > 0.89$ , the drug release mechanism is showed Case II and zero order release kinetics.<sup>19</sup>

#### Antioxidant Properties of p(AAm/TA) s-IPN and p(AAm/TA) IPN Hydrogels

To determine the total phenol and antioxidant properties of p(AAm/TA) s-IPN and p(AAm/TA) IPN hydrogels, 50 mg hydrogel was put into 40 mL of PBS (pH 7.4) at 37.5°C in a water shaker-bath for 5–7 days. Then the eluted TA released from the hydrogels were used in tests for both FC and ABTS assay methods. Also, the released TA liquid was used for antioxidant studies.

**Total Phenol Content of p(AAm/TA) s-IPN and p(AAm/TA) IPN Hydrogels.** Total phenol concentration was analyzed using the Folin-Ciocalteu (FC) method with some modifications.<sup>20</sup> Linear TA of 170 mg L<sup>-1</sup> and the release solution of TA obtained from s-IPN and IPN at 0.1 mL volume was added to 1.25 mL of 0.2 N FC phenol reagent solution and vortexed. After 4 min, 1 mL of 0.7 M Na<sub>2</sub>CO<sub>3</sub> solution was added to this mixture. After incubation for 2 h, the absorbance was measured at 760 nm with UV-VIS spectrophotometer. The antioxidant activity of the materials was expressed as ppm gallic acid equivalents.

**ABTS<sup>+</sup> Scavenging Assay.** The ABTS scavenging assay used was based on the method of Pala *et al.*<sup>20</sup> with some modification. The ABTS<sup>•+</sup> radical cation solution was prepared by incubating 2.45 mM potassium persulfate with 7 mM ABTS in water for 12–16 h in the dark. The stock solution was diluted with PBS until absorbance of  $0.7 \pm 0.05$  at 734 nm was observed using a UV-VIS spectrophotometer. Then, 10–50  $\mu$ L of sample at five concentrations were added to 2000  $\mu$ L of ABTS<sup>+</sup> solution and incubated for 6 min. The decrease in absorbance was monitored at 734 nm after 6 min. ABTS<sup>•+</sup> radical scavenging capacity was calculated using the following equation:

$$(\text{Inhibition, \%}) = [(A_{\text{blank}} - A_{\text{sample}}) / A_{\text{blank}}] \times 100 \quad (5)$$

where  $A_{\text{blank}}$  is the absorbance of the ABTS<sup>+</sup> solution without an antioxidant and  $A_{\text{sample}}$  is the absorbance of the ABTS<sup>+</sup> solution in the presence of the sample. The samples were diluted with PBS so as to give 20–80% reduction of the blank absorbance. Trolox standard solution (final concentration 0–15 mM) was prepared in PBS and assayed under the same conditions. Gallic acid (final concentration: 0–10 mM) and tannic acid (final concentration: 0–1 mM) standard solutions were used as positive control. The Trolox equivalent antioxidant capacity (TEAC) values were calculated from the slopes of the plots and expressed as “mM trolox g<sup>-1</sup> sample.”<sup>21</sup>

#### Antimicrobial Properties of p(AAm), p(AAm/TA) s-IPN, and p(AAm/TA) IPN Hydrogels

Antimicrobial effects of the hydrogels were determined using the broth-micro dilution test against three common strains of bacteria; *E. coli* ATCC 8739, *S. aureus* ATCC 6538, and *B. subtilis* ATCC 6633. Stock culture (0.1 mL) containing approximately  $10 \times 10^7$  CFU mL<sup>-1</sup> of each bacterial suspension and ~1–

100 mg of granulated sterile hydrogel were inoculated in 9.9 mL nutrient broth. The sterilization of hydrogels was realized by 2 min irradiation by UV lamp at 420 nm. Incubation was carried out at 35°C for 18–24 h. For enumeration, the cultures containing 100 mg hydrogel in each media were serially diluted  $10 \times 10^6$  fold using sterile FTS solution, and 100  $\mu$ L of each diluted sample was plated on nutrient agar and incubated for 18–24 h at 35°C, and finally, the surviving cells were counted. The culture without material was used as a control. The antimicrobial activity was determined as % reduction of the microorganism containing sample compared to the number of bacterial cells viability after contact with the control on the agar plate.<sup>22</sup>

#### Cell Culture of L929 Fibroblast Cells

L929 fibroblast cells were placed in flasks containing DMEM with L-glutamine, 10% FCS and 1% antibiotic and kept in a CO<sub>2</sub> incubator by conditioning with 5% CO<sub>2</sub> at 37°C for 48 h. To harvest the cells, the cell culture medium was discharged, and the cells were treated with trypsin-EDTA (0.5 mL per flask) for 3–4 min. Cells were then transferred into 15 mL eppendorf tubes and centrifuged at 3000 rpm for 1 min. The supernatant was discharged and the cells were used in prospect studies.

#### WST-1 Assay for Cytotoxicity

L929 fibroblast cells ( $5 \times 10^3$  cells per well) were placed in 96-well plates containing DMEM with L-glutamine, 10% FCS and 1% antibiotic. The plates were then kept in a CO<sub>2</sub> incubator (37°C in 5% CO<sub>2</sub>) for 24 h. The cell culture medium was replaced with fresh medium when the cells attached to the bottom of the plate. Then, different concentrations of p(AAm), p(AAm/TA) s-IPN, and p(AAm/TA) IPN (0, 4.6, 9.3, 18.7, 37.5, 75, and 150  $\mu$ g mL<sup>-1</sup> in aqueous solution) were placed into the wells and incubated for 4 h. For control, only medium was added to the well of the plate. Every assay was repeated three times. Following incubation under the same conditions for an additional 24 h, WST-1 (water-soluble tetrazolium salt) reagent (10  $\mu$ L) was added into each well. On incubation for 4 h at 37.5°C, the plates were immediately read with an ELISA Microplate Reader (BioTek) at 440 and 630 nm reference wavelengths.

#### Analysis of Apoptotic and Necrotic Cells

Double staining with Hoechst dye and propidium iodide (PI) was performed to quantify the number of apoptotic and necrotic cells in the culture on the basis of scoring cell nuclei. L929 fibroblast cells ( $10 \times 10^3$  cells per well) were grown in DMEM-F-12 with L-glutamine supplemented with 10% FCS and 1% penicillin-streptomycin at 37°C in 5% CO<sub>2</sub> humidified atmosphere by using 48-well plates. Cells were treated with different amounts of hydrogels (0, 4.6, 9.3, 18.7, 37.5, 75, and 150  $\mu$ g mL<sup>-1</sup>) in aqueous solution for a 24-h period. The control group consisted of cells and was treated with cell medium only. Both attached and detached cells were collected, then washed with PBS and stained with Hoechst dye 33342 (2  $\mu$ g mL<sup>-1</sup>), propidium iodide (PI; 2  $\mu$ g mL<sup>-1</sup>) and DNase free-RNase (100  $\mu$ g mL<sup>-1</sup>) for 15 min at room temperature. Then, 10–50  $\mu$ L of cell suspension was smeared onto a glass slide for examination by fluorescence microscope (Leica, Germany). The nuclei of normal cells were stained with blue fluorescence of low intensity but apoptotic cells were stained a stronger blue fluorescence by



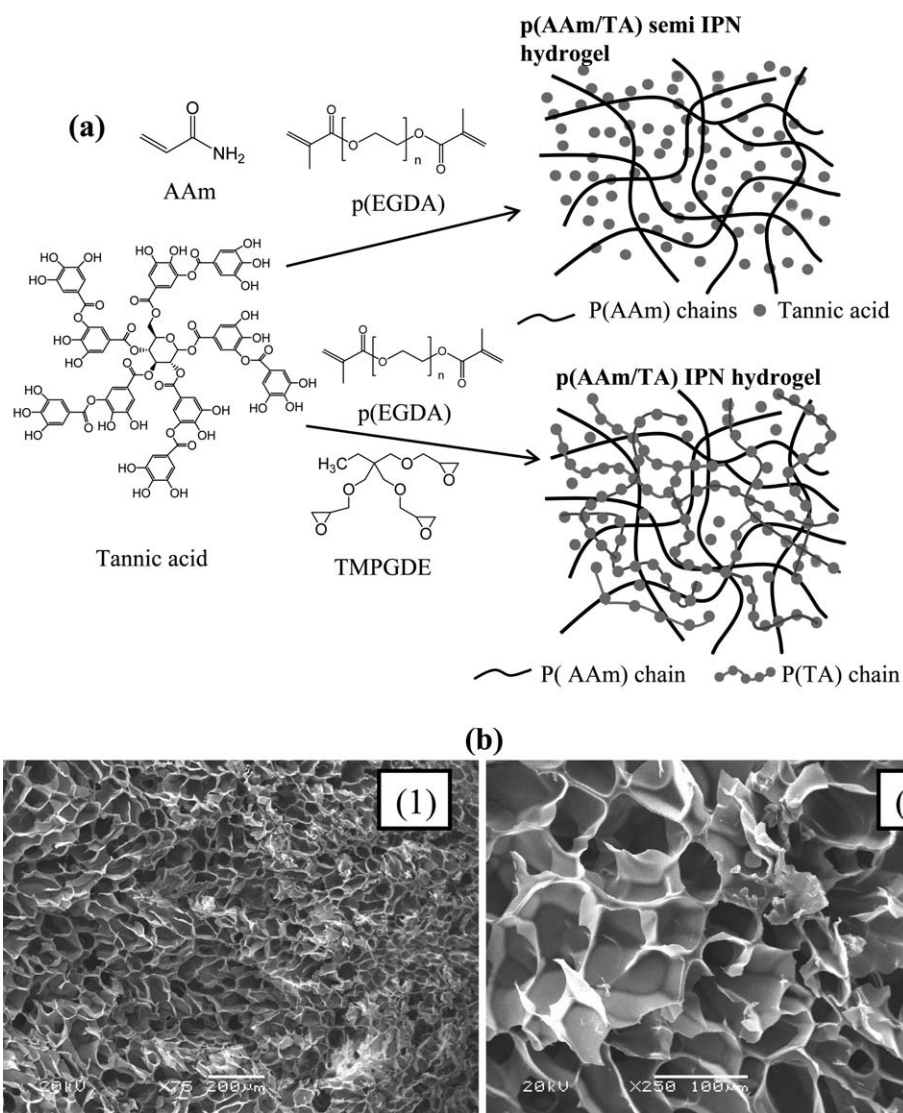


**Figure 1.** (a) Schematic representation of synthesis of p(AAm/TA) s-IPN and IPN hydrogels and (b) SEM images of (1) p(AAm/TA) s-IPN and (2) p(AAm/TA) IPN hydrogels.

the Hoechst dye. The apoptotic cells were also identified by morphological changes in the nucleus including nuclear fragmentation and chromatin condensation. Nuclei of necrotic cells were stained red by PI as PI dye can cross the cell membrane of necrotic cells lacking plasma membrane integrity. The PI dye cannot cross the non-necrotic cell membrane. The number of apoptotic and necrotic cells were counted at 10 randomly chosen microscopic fields using the 40X microscope objective. The number of apoptotic and necrotic cells were determined using a DMI600 Fluorescence Inverted Microscope (Leica, Germany) with DAPI and FITC filters, respectively. Data are expressed as a ratio of apoptotic or necrotic cells to normal cells.

## RESULTS AND DISCUSSION

### Characterization of p(AAm), p(AAm/TA) s-IPN, and p(AAm/TA) IPN Hydrogels

There is an increasing interest in preparation of effective wound healing materials with versatile properties for biological and

medical applications. Therefore, a natural polyphenol, with many medical properties, TA that is 1,2,3,4,6-pentagalloyl-glucose can be hydrolyzed under calm acidic or alkaline conditions to yield carbohydrate (glucose) and phenolic acids, gallic acid<sup>23,24</sup> was used in the preparation of p(AAm/TA) s-IPN and p(AAm/TA) IPN hydrogels and the corresponding reaction mechanisms together with their chemical formulas are shown in Figure 1(a). In the s-IPN preparation, it is clear that AAm was polymerized using p(EGDA) as crosslinker in the presence of TA to obtain p(AAm/TA) s-IPN hydrogels, where the TA molecules are almost homogeneously distributed throughout the crosslinked p(AAm) networks. On the other hand, p(AAm/TA) IPN hydrogels were synthesized by crosslinking both components, e.g., AAm monomer with p(EGDA) and TA with TMPGDE crosslinker, simultaneously. As the s-IPN contains free TA chains in comparison to IPN, it is expected to release the TA faster than IPN. Porosity is one of the most important parameters for wound dressing materials as it allows gas

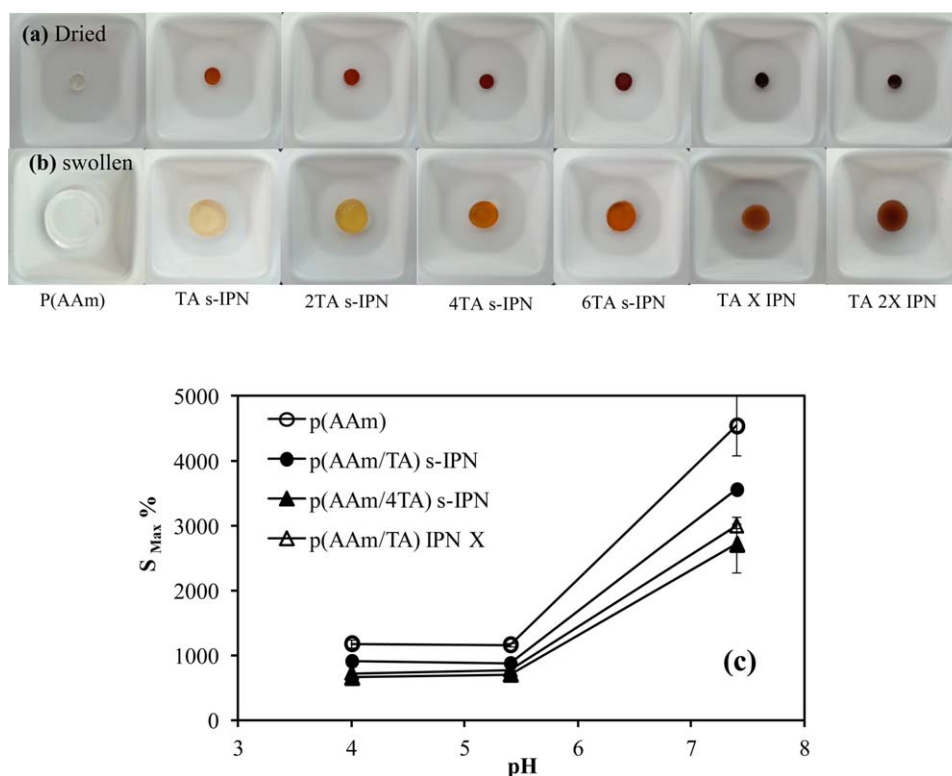


**Figure 2.** Digital camera images of (a) dried and (b) swollen p(AAm), p(AAm/TA) s-IPN, and p(AAm/TA) IPN hydrogels. (c) Maximum swelling capacity of hydrogels at different pHs (pH 4, 5.5, and 7.4) measured after 5 days. [Color figure can be viewed in the online issue, which is available at [wileyonlinelibrary.com](http://wileyonlinelibrary.com).]

exchange, e.g., of oxygen and water vapor, and permeability for other metabolites.<sup>10,11</sup> The SEM images of p(AAm/TA) IPN hydrogel are shown in Figure 1(b). It can be seen in the images that IPN hydrogels have superporous structure with size range of 50–100  $\mu\text{m}$ . The amount of used crosslinker for p(AAm) was 0.1 mol % of p(EGDA) (based on AAm) as AAm is known for its ready crosslinking property.<sup>15,16,25</sup> Therefore, in the preparation of p(AAm/TA) s-IPN hydrogel, different amounts of TA were used (to produce TA, 2TA, 4TA, and 6TA). As TA is known for its radical scavenging ability, it is expected that it can also terminate the radicals generated by APS. Therefore, to eliminate the TA inhibition effect on the gelation of s-IPN hydrogels, crosslinking amounts were also increased in the same order depending on tannic acid amount, and the initiators were doubled in comparison to virgin p(AAm) hydrogels. As can be seen from Table I, the weight of the dried p(AAm/4TA) and p(AAm/6TA) s-IPN hydrogels (containing 0.1 and 0.15 g TA) were 0.503 g and 0.440 g, suggesting that the amount of gel formed decreased when the amount of TA increased for p(AAm/4TA) and p(AAm/6TA) in s-IPN hydrogels on using the same amount of acrylamide, crosslinker and initiator. However, we also synthesized p(AAm/TA) X and p(AAm/TA) 2X IPN hydrogel containing two different amounts of crosslinker (X: crosslinker) TMPGDE to crosslink TA. As also shown in Table I, for IPN hydrogels, as the amount of crosslinker TMPGDE increased, total dried hydrogel IPN weight also increased from 0.572 to 0.625 g suggesting that TA crosslinking does occur. Moreover, the total weight of IPN hydrogel (0.572 g) was

increased compared with the s-IPN hydrogel (0.440 g) because of the crosslinking of TA molecules.

The digital camera images of dried and swollen hydrogels are illustrated in Figure 2(a). The color of the dried gels were more intense in comparison to their swollen states, and only dried and swollen p(AAm) hydrogels are transparent, implying that the other hydrogels contain colored TA. Moreover, the colors of hydrogels containing TA varied from brown to dark brown depending on the ratio of TA. p(AAm/TA) IPN is darker in comparison to p(AAm/TA) s-IPN because of the crosslinked nature of the TA molecules. On swelling of hydrogels for 3 days, p(AAm) has the highest amount of swelling but it remained colorless and transparent, whereas the swollen hydrogels of s-IPN containing TA changed their color to lighter brown and became transparent. This transparent appearance maybe useful in wound dressing materials and allow observation of the wound without removing the healing material from the surface.<sup>7</sup> However, full IPN hydrogels were not as transparent as s-IPN hydrogels and were darker than their s-IPN forms.

Another important factor for wound management is the pH, as wound liquid has a wide analytical range of pHs between 4 and 10.<sup>26</sup> There are two types of wounds; acute wounds and chronic wounds. Normally, the skin pH is 5.4, but the pH in the wound continually changes during the healing process. For acute wounds: first the acidic inflammation phase occurs with pH about 4–6, then in the second phase a more basic granulation forms, and lastly the re-epithelialization phase with {pH 4–6

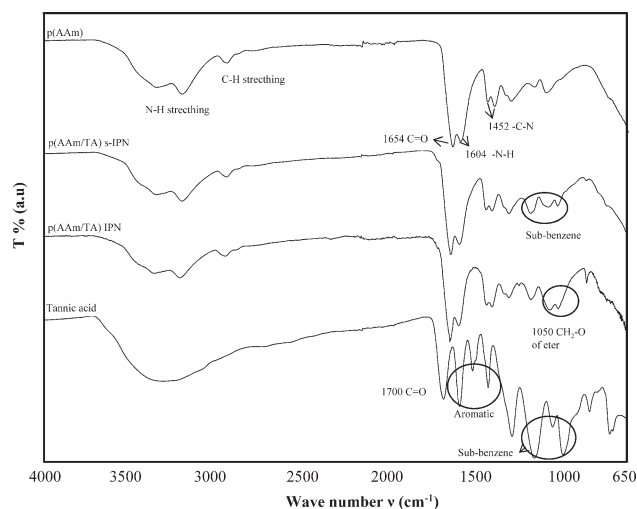


**Figure 3.** FT-IR spectra of p(AAm), p(AAm/TA) s-IPN, p(AAm/TA) IPN hydrogels, and tannic acid.

occurs. On the other hand, for chronic wounds, the pH oscillates between pH 7 and 8 as the wound fails to heal, and can decrease from 7 to 6.2.<sup>6,27</sup> For this reason, the swelling characterization of hydrogel IPN films in DI water and at various pH conditions are important for wound dressing materials. Maximum swelling of p(AAm), p(AAm/TA) s-IPN and p(AAm/TA) IPN hydrogels in different pH conditions, pH 4, 5.5, 7.4, and 9 are shown in Figure 2(b). As can be seen, bare p(AAm) hydrogels have a swelling capacity of  $4.540 \pm 454\%$  at pH 7.4 in comparison to other IPN hydrogel films. p(AAm/TA) s-IPN hydrogel has maximum swelling value of  $3.554 \pm 19\%$ , whereas p(AAm/4TA) s-IPN hydrogel has  $2.710 \pm 424\%$  maximum swelling capacity in pH 7.4 solution. With the increase in the amount of crosslinking degree of TA molecules, the swelling of hydrogels decreased. Maximum swelling capacity of p(AAm/TA) IPN was measured as  $2.994 \pm 33\%$  at pH 7.4 due to crosslinking of both components, TA and p(AAm). It can be said that p(AAm)-based hydrogels were sensitive to different pH conditions, and TA and the crosslinker amount of hydrogels determines the swelling capacity of IPN hydrogels. The swelling degree of the hydrogels increased with increasing pH of the medium. Whereas, p(AAm) based hydrogels were not well swelling related to degradation within 6h at pH 9.

For structural characterization, FT-IR spectra of p(AAm), p(AAm/TA) s-IPN, p(AAm/TA) IPN hydrogels and TA were taken, and are summarized in Figure 3. As can be seen, the characteristic peaks of the  $-\text{CONH}_2$  group of acrylamide at  $3500\text{--}3200$ ,  $2928$ ,  $1654$ ,  $1604$ , and  $1452\text{ cm}^{-1}$  are attributed to N-H bending, C-H stretching, C=O bending, N-H stretching, and  $-\text{C}-\text{N}$  stretching, respectively. TA has a broad band between  $3600$  and  $3000\text{ cm}^{-1}$  coming from  $-\text{OH}$  groups of polyphenols. The characteristic vibration peaks at  $1700\text{ cm}^{-1}$  are attributed to C=O groups for TA. The other characteristic peaks at  $1605$ ,  $1532$ , and  $1444\text{ cm}^{-1}$  can be attributed to aromatic compound stretching, and the characteristic peaks at  $1183$ ,  $1078$ , and  $1016\text{ cm}^{-1}$  are attributed to the vibration of substituted benzene rings. p(AAm/TA) s-IPN hydrogels have the

same peaks coming from the substituted benzene rings of TA molecules. However, the absorption peaks of p(AAm-TA) IPN hydrogels changed at  $1050\text{ cm}^{-1}$  corresponding to  $\text{CH}_2-\text{O}$  stretching of ether coming from the crosslinker, TMPGDE, used for the crosslinking reaction of TA for full IPN. These FT-IR peaks are the evidence of epoxy crosslinking of TA with TMPGDE via  $-\text{OH}$  groups of TA.

The thermal behavior of p(AAm) (1), p(AAm/TA) IPN (2) and p(AAm/TA) s-IPN (3) hydrogels were investigated with TG analysis and the corresponding thermograms are illustrated in Figure 4(a). p(AAm) hydrogels have two main degradation temperatures, and the weight loss started at about  $117^\circ\text{C}$  and continued up to  $221^\circ\text{C}$  with 2.2% weight loss. The degradation {between  $222$  and  $337.9^\circ\text{C}$  with 7.3% weight loss is also seen in the inset of Figure 4(a). The second main thermal degradation was between  $355$  and  $476^\circ\text{C}$  with 75.8% weight loss. p(AAm/

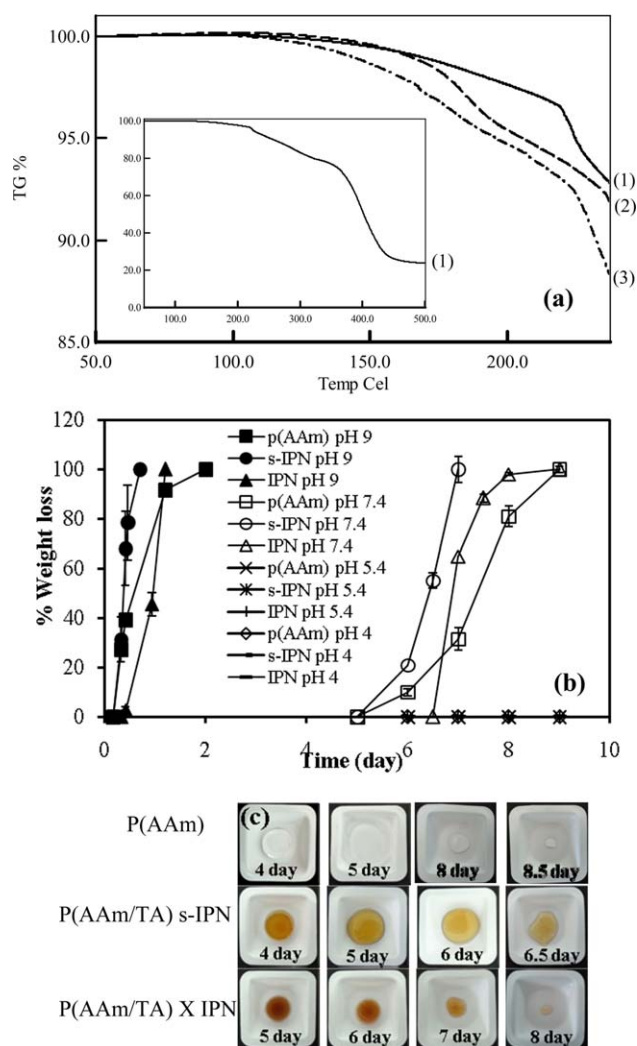


**Figure 4.** (a) TGA curves of (1) p(AAm), (2) p(AAm/TA) IPN, and (3) p(AAm/TA) s-IPN hydrogels. (b) Degradation of p(AAm), p(AAm/TA) IPN, and p(AAm/TA) s-IPN hydrogels within pH 7.4 and pH 9 at  $37.5^\circ\text{C}$  and (c) their corresponding digital camera images at pH 7.4. [Color figure can be viewed in the online issue, which is available at wileyonlinelibrary.com.]



TA) IPN and p(AAm/TA) s-IPN hydrogels have nearly the same thermal durability because of their TA content. The initial weight loss was determined between 139 and 190.7°C with 3.7% weight loss for p(AAm/TA) IPN hydrogels, and between 133 and 215°C a total of 6.5% weight loss occurred for p(AAm/TA) s-IPN hydrogels. The other degradation range was measured between 229 and 237.7°C with 8.3% weight loss for p(AAm/TA) IPN hydrogels, and between 226.7 and 237.7°C with 11.8% weight loss for p(AAm/TA) s-IPN hydrogels. All the amounts of IPN and s-IPN hydrogels were degradable at about 238°C. All the results indicate that bare p(AAm) hydrogel was thermally durable in comparison to the TA-containing IPN and s-IPN hydrogels. Also, p(AAm/TA) IPN hydrogels showed more thermal durability than s-IPN hydrogels due to the crosslinked nature of TA with TMPGDE.

Controllable biodegradation of biomaterials is very important in regulating cell proliferation and tissue regeneration for wound healing applications.<sup>28</sup> It was reported that the degradability inhibits the proliferation of keloid fibroblasts, resulting in acceleration of wound healin.<sup>18</sup> The rate of biodegradation depends mainly on the medium temperature, pH and solvents. Therefore, here we compared the degradation of hydrogels at pH 4, pH 5.4, pH 7.4 and pH 9 at 37.5°C representing physiological conditions. As illustrated in Figure 4(b), the weight loss of p(AAm), p(AAm/TA) s-IPN, and p(AAm/TA) IPN hydrogels in low pH conditions (pH 4 and pH 5.4), PBS (pH 7.4), and in basic conditions (pH 9) at 37.5°C were graphed for 1–9 days. All hydrogel types were completely degraded within 1–2 days in basic conditions (pH 9), however, the same hydrogels were degraded in PBS (pH 7.4) over a period of 6–9 days. Moreover, all types of hydrogels weren't degradable at pH 4 and pH 5.4 for 9 days. As the used crosslinkers are degradable crosslinkers for p(AAm), and even TA, the basic hydrolysis (pH 9) of the prepared hydrogels is faster in comparison to relatively neutral hydrolysis (pH 7.4). As illustrated in Figure 4(c), p(AAm)-based hydrogels were swollen in high pH conditions and then their crosslinker chains degraded via hydrolysis of ether bonds and their sizes reduced with time. As even p(AAm)-based hydrogels are degradable in high pH conditions, it is possible to control degradation rates by using higher amounts of crosslinker during hydrogel film preparation and this can be very useful for chronic wound healing pH conditions (pH 7.4). Moreover, TA containing-p(AAm/TA) s-IPN hydrogels and p(AAm/TA) IPN degradation rates are faster than p(AAm) hydrogels. Again, the used amounts of second crosslinker (TMPGDE) for TA can also be tuned to control the degradation rate of the IPN. As a result, the existence of TA increases the degradation of hydrogel networks whether it is s-IPN or IPN. Comparing s-IPN with IPN hydrogels, the weight loss of IPN hydrogels was measured as 45.7% after 1 day whereas s-IPN hydrogels have 100% weight loss after 1 day in pH 9 at 37.5°C. IPN hydrogel was more durable than s-IPN hydrogel because TA was crosslinked with TMPGDE in the IPN hydrogel structure.

The zeta potential of hydrogels is also a very important parameter in biological fluids of acute wounds. The electrical charge of skin continually changes, as the skin pH isn't stable at the contact with injured tissue.<sup>29–31</sup> Thus, the change in zeta potential

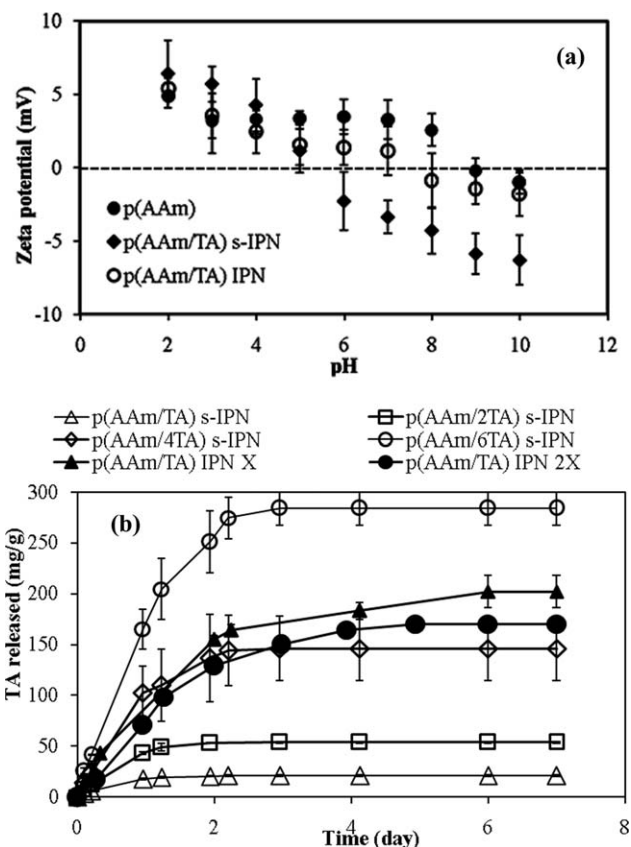


**Figure 5.** (a) Zeta potentials (mV) of p(AAm), p(AAm/TA) s-IPN and p(AAm/TA) IPN hydrogels in 0.01 M KCl solutions in DI water at different pH values between 2 and 10. (b) TA release profiles from p(AAm/TA) IPN, and p(AAm/TA) s-IPN hydrogel in PBS (pH 7.4) at 37.5°C.

at different pH conditions for the prepared hydrogels were investigated. Zeta potentials (mV) of granulated p(AAm), p(AAm/TA) s-IPN and p(AAm/TA) IPN hydrogels in 0.01 M KCl solutions at different pH values ranging from 2 to 10 were measured and are given in Figure 5(a). The surface charge and iso-electronic point of the materials were dependent on the pH of the medium. The surface charge of p(AAm) changed from  $4.9 \pm 0.8$  to  $-1 \pm 0.8$  mV in the pH range of 2–10 owing to the many  $-C(O)NH_2$  groups, and the zero charge (iso electric point) was at about pH 9. Electrical charge of p(AAm/TA) s-IPN and IPN hydrogels were influenced by both components of the hydrogels; AAm and TA molecules. The surface charge of p(AAm/TA) IPN hydrogel was slightly increased compared to p(AAm) owing to the crosslinked TA content which has many ionizable  $-OH$  groups in the structure. The zeta potential of p(AAm/TA) s-IPN hydrogel was determined between  $6.4 \pm 2.3$  and  $-6.3 \pm 1.7$  mV in the pH range of 2–10. As can be seen from the measurements, the surface charge of s-IPN was positive at pH < 5 conditions owing to protonation of  $-NH_2$  groups coming from AAm; on the other hand, it has negatively charged character at pH > 5 conditions attributed to ionization of  $-OH$  groups coming from TA. The isoelectric points for s-IPN and IPN were measured at about pH 5 and 8, respectively. Therefore, it can be said that the surface charge of hydrogels decreased with the increase in pH of the solution.



**Table II.** Application of Various Models for TA Release from p(AAm/TA) Based Materials

Hydrogel	Zero order		First order		Korsmeyer-Peppas	
	$k_0$ (g day <sup>-1</sup> )	$R^2$	$k$ (day <sup>-1</sup> )	$R^2$	$n$	$R^2$
p(AAm/TA) s-IPN	33.36 ± 2.9	0.938	0.28 ± 0.01	0.917	0.70 ± 0.02	0.998
p(AAm/2TA) s-IPN	40.43 ± 4.8	0.906	0.32 ± 0.02	0.956	0.79 ± 0.03	0.999
p(AAm/4TA) s-IPN	33.67 ± 1.7	0.938	0.27 ± 0.02	0.985	0.86 ± 0.02	0.995
p(AAm/6TA) s-IPN	36.59 ± 5.6	0.966	0.30 ± 0.04	0.997	0.85 ± 0.04	0.997
p(AAm/TA) X IPN	27.28 ± 2.2	0.990	0.19 ± 0.02	0.999	1.11 ± 0.02	0.999
p(AAm/TA) 2X IPN	27.93 ± 1.8	0.980	0.17 ± 0.01	0.994	0.82 ± 0.01	0.989

### Tannic Acid Release Studies from s-IPN and IPN Hydrogels

Phenolic compounds can be used as bioactive materials and hydrogel IPN containing TA and/or other phenolic compounds can be suitable as wound dressing materials for chronic wound treatment.<sup>32</sup> As demonstrated in Figure 5(b), the capability of p(AAm/TA) IPN hydrogels, which have different amount of crosslinkers (X and 2X) and p(AAm/TA), and s-IPN hydrogels which have four different amounts of TA (TA, 2TA, 4TA, and 6TA), to release TA were compared. In Figure 5(b), p(AAm/TA) s-IPN hydrogels containing TA, 2TA, 4TA, and 6TA released 21 ± 0.6, 54 ± 0.8, 146 ± 31, and 284 ± 16 mg g<sup>-1</sup> TA, respectively, within about 3 days. As shown in Figure 5(b), the amount of released TA is more than the amount of loaded TA per gram of hydrogel matrices. However, as given in Table I, the TA amount included in 1 g AAm was about 150 mg before polymerization. On polymerization, the weight of the obtained hydrogels including TA were always less than 1 g for example, the weight of the obtained p(AAm/6TA) s-IPN was 0.440 g. Assuming all the TA is included in the hydrogel matrices, some of the AAm monomer cannot be polymerized due to radical scavenging ability of TA. Therefore, this sample, p(AAm/6TA) s-IPN can be assumed to have about 0.341 g TA g<sup>-1</sup> gel matrices. Therefore, from the release studies, the released amount of TA was found to be 284 ± 16 mg g<sup>-1</sup> TA, that is more than the amount of TA incorporated during hydrogel s-IPN preparation. Depending on the amount of TA within s-IPNs, a linear TA release profile was obtained for one to three days, e.g., p(AAm/TA) s-IPN provides one day-long linear release profile whereas p(AAm/6TA) s-IPN provides a 3-day long release profile with almost 13.5-fold more TA released. Furthermore, the released amount of TA from p(AAm/TA) X and 2X IPN hydrogels were 202 ± 15 and 170 ± 1.4 mg g<sup>-1</sup> within 6 days, again with linear release profile up to 2 days. Due to the crosslinked nature of TA, i.e., the increased amount of TMPGDE as TA crosslinker, the total amount of TA released decreased. The greater the amounts of crosslinker used for TA, the less the amount of TA released. However, as the crosslinker is degradable over the longer release time, higher amounts of TA can be obtained from the highly crosslinked structures. All these results confirm that the presented IPN structure can be appropriately chosen for desired amounts of release of TA from the wound dressing materials. Considering the bio-usefulness of TA with antioxidant, antibacterial and anticancer nature, the IPN films prepared here have great potential in biomedical fields for versatile use including as wound dressing materials.

**TA Release Study.** For the release of TA molecules, zero order and first order kinetic models were applied and the rate constant values together with their coefficient of determination ( $R^2$ ) is given Table II. As can be seen, the TA release from p(AAm/TA) based hydrogels fits better with the first order reaction kinetic with  $R^2$  values and can be represented better Korsmeyer-Peppas model owing to their high  $R^2$  values ranging from 0.989 to 0.999. For Korsmeyer-Peppas model, the diffusional exponent values " $n$ " for all hydrogel materials were ranged from 0.7 to 0.85, with the exception of the  $n$  values of p(AAm/TA) 2X IPN hydrogels that were found as 1.11. Thus, all hydrogels have anomalous or non-Fickian diffusion mechanism except for p(AAm/TA) 2X IPN hydrogels which shows case II transport mechanism and zero order kinetics.

### Antioxidant Activity of p(AAm), p(AAm-TA) IPN and s-IPN Hydrogels

Phenolic antioxidant agents can be used for continuous quenching of free radicals to heal chronic wounds.<sup>33</sup> Tannic acid is known as an antioxidant agent and the strength is dependent on the concentration and free radical source.<sup>34</sup> For antioxidant properties of p(AAm/TA) s-IPN and p(AAm/TA) IPN, FC, and ABTS assay methods were used and their results are shown in Table III. The ABTS radical scavenging activity of GA and TA were determined with two common antioxidants as standard for comparison of the antioxidant potential of IPNs. As shown in Table II, 170 mg L<sup>-1</sup> TA molecules had 140 ± 5 mg L<sup>-1</sup> GA equivalency. The total phenol content and antioxidant properties of p(AAm/TA) IPN and s-IPN hydrogels were determined from their TA released solution in PBS. p(AAm/TA) IPN X hydrogel has antioxidant equivalency of 149 ± 17 mg L<sup>-1</sup> GA, but s-IPN hydrogels containing TA, 2TA, 4TA, and 6TA, have antioxidant equivalency of 53 ± 11, 89 ± 20, 122 ± 5, and 171 ± 12 mg L<sup>-1</sup> of GA. This is a clear demonstration that total phenol contents increased depending on the TA amount in s-IPN. Additionally, the antioxidant effects of p(AAm/TA) IPN and s-IPN hydrogels were determined by ABTS radical scavenging methods. TEAC value of antioxidant materials was measured with various concentrations of samples that cause % scavenging capability of certain ABTS radicals. TEAC values of GA and TA, which were used as controls, were 2.48 ± 0.3 and 21.64 ± 0.4 mM trolox g<sup>-1</sup>. The TEAC values of p(AAm/TA) IPN X hydrogel was determined as 564 ± 0.5, whereas s-IPN hydrogels containing TA, 2TA, 4TA, and 6TA have 376 ± 0.1, 449 ± 0.1, 522 ± 0.2 and 597 ± 0.4 mM trolox g<sup>-1</sup>. The results

**Table III.** The Comparison of Antioxidant Capability of p(AAm/TA) s-IPN and p(AAm/TA) IPN with Gallic Acid (GA) and Free TA to Determine Their Total Phenol Content, and TEAC (Trolox Equivalent Antioxidant Capacity) Values

	GA	TA	6TA s-IPN	4TA s-IPN	2TA s-IPN	TA s-IPN	TA X IPN
Total phenol content <sup>a</sup> ( $\mu\text{g mL}^{-1}$ )	-	140 ± 5	171 ± 12	122 ± 5	89 ± 20	53 ± 11	149 ± 17
TEAC value (mM trolox equivalent $\text{g}^{-1}$ )	2.48 ± 0.4	21.64 ± 0.4	597 ± 0.4	522 ± 0.2	449 ± 0.1	376 ± 0.1	564 ± 0.5

<sup>a</sup> 170  $\mu\text{g mL}^{-1}$  linear TA and TA released solution of hydrogels expresses as  $\mu\text{g mL}^{-1}$  gallic acid equivalency.

presented in Table II indicate that the antioxidant effect of IPN hydrogel was lower than s-IPN hydrogel possibly due to the crosslinked nature of TA with TMPGDE as crosslinker, where some of the crosslinker also releases with TA. It is important to note that p(AAm) hydrogel showed no antioxidant properties. However, all these antioxidant tests confirm that these IPN films have some antioxidant properties that protect wounds or open scars from infection and diseases where antioxidant capability plays a significant role.

#### Antimicrobial Properties of p(AAm), p(AAm/TA) s-IPN, and p(AAm/TA) IPN Hydrogels

Microorganisms, fungi or bacteria exist as about  $10^6$  organisms per gram of tissue.<sup>34,35</sup> Previous studies reported that tannic acid is a natural antimicrobial molecule against many bacteria strains.<sup>36</sup> Here, the synthesized TA-containing hydrogel IPN materials were tested for their antimicrobial capabilities. The antimicrobial activity of p(AAm), p(AAm/TA) s-IPN, and p(AAm/TA) IPN hydrogels were evaluated by broth-micro dilution test against three common bacteria species; *E. coli* ATCC 8739 (gram-negative), *S. aureus* ATCC 6538 (gram-positive), and *B. subtilis* ATCC 6633 (gram-positive). The reduction of microorganism (%) against 10  $\text{mg mL}^{-1}$  of the hydrogels, and TA molecules are summarized in Table IV. As can be seen, for

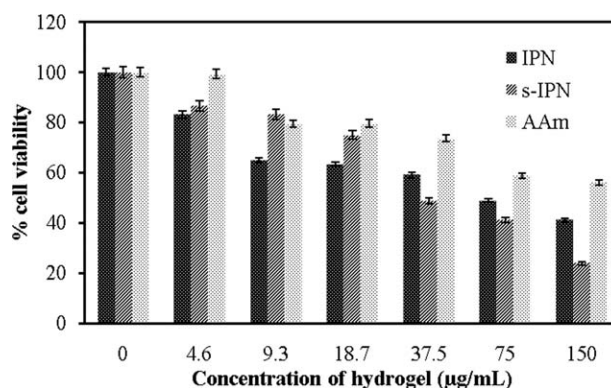
**Table IV.** The Reduction % of Microorganisms for 10  $\text{mg mL}^{-1}$  of p(AAm) and Tannic Acid-Based Materials Against *Escherichia coli* ATCC 8739, *Staphylococcus aureus* ATCC 6538, and *Bacillus subtilis* ATCC 6633 Strains

Antimicrobial materials		The reduction % of organisms
p(AAm)	<i>B. subtilis</i>	0
	<i>S. aureus</i>	0
	<i>E. coli</i>	0
p(AAm/6TA) s-IPN	<i>B. subtilis</i>	61.4 ± 5.0
	<i>S. aureus</i>	76.6 ± 4.0
	<i>E. coli</i>	56.7 ± 6.0
p(AAm/TA) X IPN	<i>B. subtilis</i>	38.5 ± 3.0
	<i>S. aureus</i>	72.2 ± 5.0
	<i>E. coli</i>	13.5 ± 3.0
TA	<i>B. subtilis</i>	76.8 ± 4.0
	<i>S. aureus</i>	88.3 ± 5.0
	<i>E. coli</i>	74.2 ± 4.0

p(AAm) hydrogel no antimicrobial effects were observed. For control studies, the % reduction of organisms for TA were found to be 76.8%, 88.3%, and 74% against *B. subtilis*, *S. aureus*, and *E. coli*, respectively. The cell wall of the gram-negative bacteria consists of lipids, proteins and lipopolysaccharides that provide effective protection against biocides whereas the gram-positive bacteria does not contain lipopolysaccharides.<sup>26</sup> Therefore, the gram-negative bacteria, *E. coli*, is less sensitive to TA molecules compared with gram-positive bacteria such as *S. aureus* and *B. subtilis*. However, the reduction of organisms (%) for s-IPN ( $\sim 10$  mg) was 61.4%, 76.6%, and 56.7% whereas the IPN hydrogel (weighing  $\sim 10$  mg) showed 38.5, 72.2, and 13.5% reductions in for *B. subtilis*, *S. aureus*, and *E. coli* microorganisms, respectively. It is clear that s-IPN hydrogels are more effective than IPN hydrogels, again due to the crosslinked nature of TA molecules in the IPN hydrogel network, and thus the released TA molecules may have some crosslinker attached to them.

#### Cytotoxicity Test for p(AAm), p(AAm/TA) s-IPN, and p(AAm/TA) IPN Hydrogel Films

Previously in a study it was shown that TA crosslinked collagen scaffolds were biocompatible with 3T3 fibroblast cells and shown to promote wound healing by aiding the closure of the wound due to the resistance of the collagen scaffold to enzymes,<sup>37</sup> therefore, in this study, p(AAm), p(AAm/TA) s-IPN, and p(AAm/TA) IPN were tested against L929 fibroblast cells to determine their biocompatibility, and the results are given in Figure 6. As can be seen from Figure 6, it can be assumed that all the studied hydrogels in this investigation up to almost 20  $\mu\text{g mL}^{-1}$  concentration are biocompatible with about 75% cell

**Figure 6.** Cytotoxicity of p(AAm), p(AAm/TA) s-IPN, and IPN hydrogels with varying concentrations (0–150  $\mu\text{g mL}^{-1}$ ) for L929 fibroblast cell.

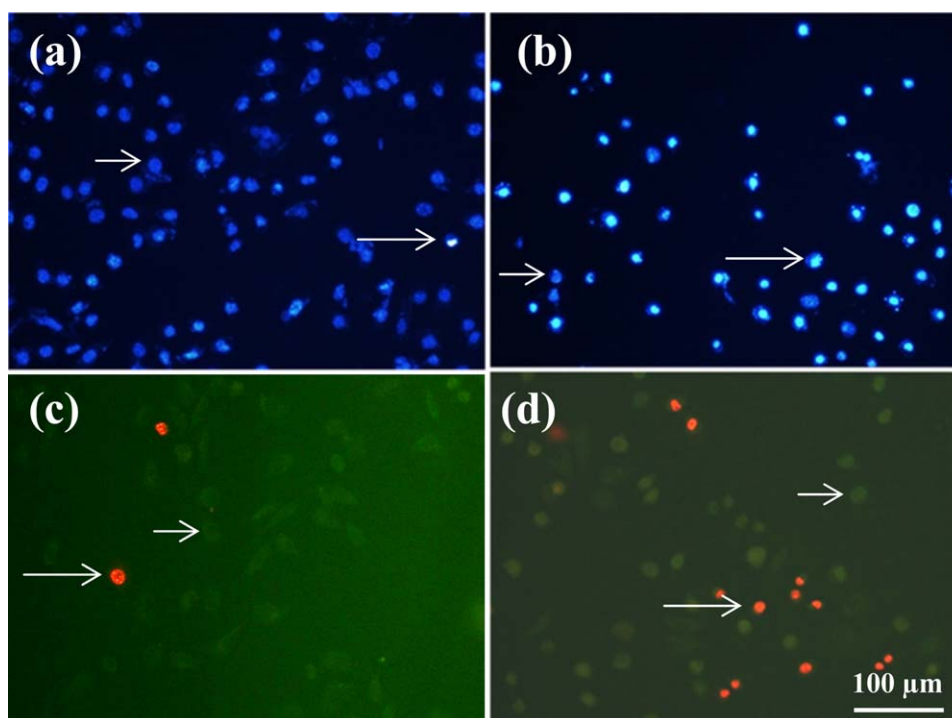


**Figure 7.** Inverted microscopy images of apoptotic and necrotic cells by using double staining performed with Hoechst 33342 and propidium iodide (PI) fluorescent stains. (a) L929 fibroblast cells stained by Hoechst 33342 (control group), nuclei look blue (short arrows). (b) L929 fibroblast cells stained by Hoechst 33342; some of the cells (long arrows) were exposed to apoptosis as a result of their interaction with IPN in the concentration of 150  $\mu\text{g/mL}$ . (c) Image of L929 fibroblast cells stained by Hoechst 33342 and PI interacted with only medium (control group), non-necrotic cells look green. (d) Image of L929 fibroblast cells interacted with s-IPN at 37.5  $\mu\text{g/mL}$ ; necrosed cell nuclei look red (long arrows) stained with PI and non-necrosed cell nuclei look green (stained by Hoechst 33342). [Color figure can be viewed in the online issue, which is available at [wileyonlinelibrary.com](http://wileyonlinelibrary.com).]

viability. It is also clear that % viability decreases with the increase in amount of hydrogel grains. It can be said that the order of biocompatibility over 18.7  $\mu\text{g mL}^{-1}$  concentration is in the order of p(AAm) > IPN > s-IPN and below this concentration only IPN and s-IPN are swapped, again this can be attributed to the chemically crosslinked nature of TA. Therefore, it can be assumed that around 18.7–37  $\mu\text{g mL}^{-1}$  particle concentration can be assumed viable for L929 fibroblast cells. The cell viability was tested according to the literature with some modification and with hydrogels ground into smaller pieces, about 50  $\mu\text{m}$  visualized by optical microscope. There are similar results also reported in the literature, e.g., p(sucrose) micro particles were investigated for cytotoxicity against fibroblast cells, and it was reported that p(sucrose) micro particles were about 26% cytotoxic to fibroblast cells at concentration range of 100  $\mu\text{g mL}^{-1}$ .<sup>38,39</sup>

#### Double Staining Result

The apoptotic and necrotic effects of p(AAm), s-IPN and IPN on L929 fibroblast cell lines were investigated. The results of the apoptotic and necrotic indices are given in Table IV, and the double staining images are given in Figure 7. The apoptotic and necrotic indices were determined by taking the average values obtained by the double staining method. Figure 7(a,b) were taken under DAPI filter, while (c) and (d) were taken under FITC filter. For apoptotic index, the fibroblast cell nucleus was stained with Hoechst 33342. Inverted fluorescent microscope

images of control group nuclei were homogenous and blue in color [Figure 7(a)], whereas, the apoptotic cell nucleus decomposed and appeared brighter blue in color compared to non-apoptotic cells under fluorescent light [Figure 7(b)]. As can be seen from Table IV, the apoptotic effect of hydrogels was increased with the increase in concentration. The highest apoptotic index was 15% for IPN hydrogels at 150  $\mu\text{g mL}^{-1}$  concentration, and as shown in Figure 7(a,b), the nuclei color for the control groups was blue (short arrow), but the apoptotic cell nuclei of IPN hydrogel in the concentration of 150  $\mu\text{g mL}^{-1}$  appeared bright blue (long arrow) in color as shown in Figure 7(b). The s-IPN showed lower apoptotic indices, with  $11 \pm 0.5$  for 150  $\mu\text{g mL}^{-1}$  concentration.

For necrotic cells, the fibroblast cell nucleus was stained with propidium iodide (PI). Propidium iodide penetrates the damaged cell and dyes the membrane. The necrotic cell nuclei appeared red in color whereas the live cells were green, and the image of L929 fibroblast cells interacted with s-IPN at 37.5  $\mu\text{g mL}^{-1}$ ; necrosed cell nuclei assumed a red color (long arrows) stained with PI and non-necrosed cell nuclei assumed a green color as given in Figure 7(c,d). The % necrotic index is given in Table V, and the image of necrotic cells are shown in Figure 7(c,d). According to Table V, the low necrotic index of hydrogels were found at low concentrations between 4.6 and 18.75  $\mu\text{g mL}^{-1}$ . Especially, 18.75  $\mu\text{g mL}^{-1}$  concentration of p(AAm) showed a necrotic index of about 8.5%. At high concentrations



**Table V.** Apoptotic and Necrotic Indices for L929 Fibroblast Cells Measured at Varying Concentrations (0–150  $\mu\text{g mL}^{-1}$ )

Concentration of hydrogel ( $\mu\text{g mL}^{-1}$ )	TA X IPN		6TA s-IPN		p(AAm)	
	% apoptosis	% necrosis	% apoptosis	% necrosis	% apoptosis	% necrosis
0	1.0 $\pm$ 1.0	1.0 $\pm$ 0.5	1.0 $\pm$ 1.0	1.0 $\pm$ 0.5	1.0 $\pm$ 1.0	1.0 $\pm$ 0.5
4.6	5.0 $\pm$ 0.5	15.0 $\pm$ 1.0	4.5 $\pm$ 0.8	13.5 $\pm$ 1.0	4.0 $\pm$ 1.4	1.5 $\pm$ 1.0
9.37	7.0 $\pm$ 1.0	22.5 $\pm$ 2.0	6.0 $\pm$ 1.5	16.0 $\pm$ 0.7	6.5 $\pm$ 1.0	5.0 $\pm$ 0.7
18.75	8.0 $\pm$ 0.7	25.5 $\pm$ 1.0	7.0 $\pm$ 2.0	22.0 $\pm$ 0.5	7.0 $\pm$ 0.7	8.5 $\pm$ 2.0
37.5	8.5 $\pm$ 2.0	27.0 $\pm$ 0.8	8.0 $\pm$ 1.2	28.5 $\pm$ 2.0	8.5 $\pm$ 2.0	15.0 $\pm$ 1.4
75	10.0 $\pm$ 1.4	32 $\pm$ 0.5	9.5 $\pm$ 1.0	30.0 $\pm$ 0.8	9.0 $\pm$ 1.5	23.5 $\pm$ 1.0
150	15.0 $\pm$ 0.6	39.5 $\pm$ 1.0	11 $\pm$ 0.5	34.5 $\pm$ 1.0	13.0 $\pm$ 2.0	30.0 $\pm$ 1.5

of all hydrogels, the necrotic indices increased. Particularly, 150  $\mu\text{g mL}^{-1}$  concentration of p(AAm/TA) IPN was determined to generate about 39.5  $\pm$  1.0% necrotic index. As illustrated in Figure 7(c,d), the nuclei color for control groups was green (short arrow), however, the necrotic cell nuclei with 150  $\mu\text{g mL}^{-1}$  of IPN hydrogel concentration appeared red in color.

All the results show that IPN hydrogel has higher apoptotic and necrotic effects compared with p(AAm) and s-IPN hydrogels against L929 fibroblast cells. Interestingly, p(AAm) hydrogel has the lowest % apoptotic and necrotic cells at low and high concentrations of hydrogels implying that IPN hydrogels release TA and play a significant role in the apoptosis and necrosis of the L929 fibroblast cells. Therefore, IPNs with tunable TA concentration maybe useful for interesting drug delivery devices in multifunctional wound dressing materials

## CONCLUSIONS

In this investigation, novel p(AAm/TA) s-IPN and IPN hydrogel films were readily prepared from AAm monomer and natural polyphenol, TA, via redox polymerization and concomitant epoxy crosslinking technique, respectively. The prepared hydrogels were demonstrated to be resourceful as biodegradable wound dressing films with inherently releasing active therapeutic agent (TA releasing) and different choices of preparation methods such as semi-IPN or full IPN with variable TA contents. All the prepared hydrogels in this investigation are fully degradable in about 6–9 days in PBS (pH 7.4) at 37.5°C. Moreover, by adjusting the amount of TA and/or morphology of hydrogel films containing TA such as s-IPN and IPN, the TA and/or active agent release profile can be regulated to meet the demands of different wound healing applications. It was further demonstrated that the synthesized p(AAm/TA) s-IPN and IPN hydrogels are effectively antioxidant materials, and were found to be antimicrobial against three common bacteria [*E. coli* ATCC 8739 (gram-negative), *S. aureus* ATCC 6538 (gram-positive), and *B. subtilis* ATCC 6633 (gram-positive) at relatively high concentrations, above 100  $\text{mg mL}^{-1}$ ] due to amenable TA contents. For example, released amounts of TA from IPN hydrogel shows linear release profiles up to 3 days, and can be controlled by appropriate design of the IPN. In addition, at lower concentrations, 18.7–37  $\mu\text{g mL}^{-1}$ , the prepared hydrogel films can be considered as biocompatible for L929 fibroblast

cells and showed acceptable apoptotic and necrotic indices at this concentration. Therefore, these kinds of wound dressing material can be used for real applications and play a significant role in the healing of many wounds, such as burns, chronic, and acute wounds.

## ACKNOWLEDGMENTS

The authors are grateful to Prof. Nurettin Sahiner for providing great support in carrying out most of the experiments; also, the authors are grateful to Prof. Mustafa Turk for biocompatibility experiments.

## REFERENCES

- Mogosanu, G. D.; Grumezescu, A. M. *Int. J. Pharm.* **2014**, *463*, 127.
- Ito, T.; Yoshida, C.; Murakami, Y. *Mater. Sci. Eng. C* **2013**, *33*, 3697.
- Bartolotta, A.; Marco, G. D.; Lanza, M.; Carini, G.; D'Angelo, A.; Tripodo, G.; Fainleib, A.; Danilenko, I.; Grytsenko, V.; Sergeeva, L. *Mater. Sci. Eng. A* **2004**, *370*, 288.
- Dragan, E. S. *Chem. Eng. J.* **2014**, *243*, 572.
- George, B. P.; Parimelazhagan, T.; Chandran, R. *Ind. Crop. Prod.* **2014**, *54*, 216.
- Schneider, L. A.; Korber, A.; Grabbe, S.; Dissemond, J. *Arch. Dermatol. Res.* **2007**, *298*, 413.
- Boateng, J. S.; Matthews, K. H.; Stevens, H. N. E.; Eccleston, G. M. *J. Pharm. Sci.* **2008**, *97*, 2892.
- Perez, D.; Bramkamp, M.; Exe, C.; von Ruden, C.; Ziegler, A. *Am. J. Surg.* **2010**, *199*, 14.
- Liakos, I.; Rizzello, L.; Scurr, D. J.; Pompa, P. P.; Bayer, I. S.; Athanassiou, A. *Int. J. Pharm.* **2014**, *463*, 137.
- Wijekoon, A.; Fountas-Davis, N.; Leipzig, N. D. *Acta Biomater.* **2013**, *9*, 5653.
- Altiok, D.; Altiok, E.; Tihminlioglu, F. *J. Mater. Sci. Mater. Med.* **2010**, *21*, 2227.
- Tikoo, K.; Bhatt, D. K.; Gaikwad, A. B.; Sharma, V.; Kabra, D. G. *FEBS Lett.* **2007**, *581*, 2027.

13. Orłowski, P.; Krzyżowska, M.; Zdanowski, R.; Winnicka, A.; Nowakowska, J.; Stankiewicz, W.; Tomaszewska, E.; Celichowski, G.; Grobelny, J. *Toxicol. In Vitro* **2013**, *27*, 1798.
14. Khan, N. S.; Ahmad, A.; Hadi, S. M. *Chem. Biol. Interact.* **2000**, *125*, 177.
15. Kılıç, G.; Malcı, S.; Çelikbıçak, O.; Sahiner, N.; Salih, B. *Anal. Chim. Acta* **2005**, *547*, 18.
16. Sagbas, S.; Sahiner, N. *Fuel Process Technol.* **2012**, *104*, 31.
17. Seven, F.; Sahiner, N. *Int. J. Hydrogen Energy* **2013**, *38*, 777.
18. Yang, C.; Xu, L.; Zhou, Y.; Zhang, X.; Huang, X.; Wang, M.; Han, Y.; Zhai, M.; Wei, S.; Li, J. *Carbohydr. Polym.* **2010**, *82*, 1297.
19. Costa, P.; Lobo, J. M. S. *Eur. J. Pharm. Sci.* **2001**, *13*, 123.
20. Fiol, M.; Weckmüller, A.; Neugart, S.; Schreiner, M.; Rohn, S.; Krumbein, A.; Kroh, L. W. *Food Chem.* **2013**, *138*, 857.
21. Pala, C. U.; Toklucu, A. K. *J. Food Comp. Anal.* **2011**, *24*, 790.
22. Zemljić, L. F.; Peršin, Z.; Stenius, P. *Biomacromolecules* **2009**, *10*, 1181.
23. Bozic, M.; Gorgieva, S.; Kokol, V. *Carbohydr. Polym.* **2012**, *89*, 854.
24. Chen, G.; Niu, C.; Zhou, M.; Ju, X.; Xie, R.; Chu, L. *J. Colloid Interface Sci.* **2010**, *343*, 168.
25. Sahiner, M.; Butun, S.; Alpaslan, D.; Bitlisli, B. O. *Hacettepe J. Biol. Chem.* **2014**, *42*, 63.
26. Sharp, D. *Biosens. Bioelectron.* **2013**, *50*, 399.
27. Dargaville, T. R.; Farrugia, B. L.; Broadbent, J. A.; Pace, S.; Upton, Z.; Voelcker, N. H. *Biosens. Bioelectron.* **2013**, *41*, 30.
28. Huang, X.; Zhang, Y.; Zhang, X.; Xu, L.; Chen, X.; Wei, S. *Mater. Sci. Eng. C* **2013**, *33*, 4816.
29. Hebeish, A.; El-Rafiea, M. H.; EL-Sheikha, M. A.; Seleemb, A. A.; El-Naggar, M. E. *Int. J. Biol. Macromol.* **2014**, *65*, 509.
30. Nistor, M. T.; Chiriac, A. P.; Nita, L. E.; Vasile, C. *Int. J. Pharm.* **2013**, *452*, 92.
31. Farber, P. L.; Hochman, B.; Furtado, F.; Ferreira, L. M. *Med. Hypotheses* **2014**, *82*, 199.
32. Rocasalbas, G.; Francesco, A.; Tourino, S.; Fernández-Francos, X.; Guebitz, G. M.; Tzanov, T. *Carbohydr. Polym.* **2013**, *92*, 989.
33. Nyanhongo, G. S.; Sygmund, C.; Ludwig, R.; Prasetyo, E. N.; Guebitz, G. M. *Eur. J. Pharm. Biopharm.* **2013**, *83*, 396.
34. Labieniec, M.; Gabryelak, T.; Falcioni, G. *Mutat. Res.* **2003**, *539*, 19.
35. Robson, M. C.; Heggors, J. P. *Mil. Med.* **1969**, *134*, 19.
36. Robson, M. C.; Stenberg, B. D.; Heggors, J. P. *Clin. Plast. Surg.* **1990**, *17*, 485.
37. Kim, T. J.; Silva, J. L.; Kim, M. K.; Jung, Y. S. *Food Chem.* **2010**, *118*, 740.
38. Natarajan, V.; Krithica, N.; Madhan, B.; Kumar, P. *J. Biomed. Mater. Res. Part B* **2013**, *101*, 560.
39. Sahiner, N.; Sagbas, S.; Turk, M. *Int. J. Biol. Macromol.* **2014**, *66*, 236.